Characterizations of low-temperature electroluminescence from ZnO nanowire light-emitting arrays on the *p*-GaN layer

Tzu-Chun Lu,[1] Min-Yung Ke,[1] Sheng-Chieh Yang,[1] Yun-Wei Cheng,[1] Liang-Yi Chen,[1] Guan-Jhong Lin,[1] Yu-Hsin Lu,[2] Jr-Hau He,[1,3] Hao-Chung Kuo,[2] and JianJang Huang[1,3,*]

[1]*Graduate Institute of Photonics and Optoelectronics, National Taiwan University, 1, Roosevelt Road, Sec. 4, Taipei 106, Taiwan*

[2]*Department of Photonics, National Chiao Tung University, Hsinchu 300, Taiwan*

[3]*Department of Electrical Engineering, National Taiwan University, 1, Roosevelt Road, Sec. 4, Taipei 106, Taiwan*

**Corresponding author: jjhuang@cc.ee.ntu.edu.tw*

Received August 24, 2010; revised November 3, 2010; accepted November 4, 2010; posted November 10, 2010 (Doc. ID 133811); published December 6, 2010

Low-temperature electroluminescence from ZnO nanowire light-emitting arrays is reported. By inserting a thin MgO current blocking layer in between ZnO nanowire and *p*-GaN, high-purity UV light emission at wavelength 398 nm was obtained. As the temperature is decreased, contrary to the typical GaN-based light emitting diodes, our device shows a decrease of optical output intensity. The results are associated with various carrier tunneling processes and frozen MgO defects. © 2010 Optical Society of America

OCIS codes: 230.3670, 230.5590, 240.7040, 260.7190.

ZnO-based nanostructures have been explored for potential applications to light-emitting devices. Vertically aligned ZnO nanowires can be synthesized with various low-temperature methods including electrodeposition [1], spray pyrolysis [2], vapor deposition method [3], and hydrothermal synthesis [4]. Recently, several research projects have demonstrated nanowire light-emitting diodes (LEDs) consisting of a *p*-type GaN thin film and *n*-type ZnO vertical nanowire arrays [5–8]. However, in most works the defect band emission was observed in the electroluminescence (EL) spectra. Similar behavior can be observed from planar devices with the ZnO thin film on *p*-GaN [9], which is associated with the carrier overflow to the bulk semiconductor without radiatively recombining in the depletion region in the heterojunction [10]. To mitigate defect band emission, a high-bandgap MgO is proposed in this Letter as the carrier blocking layer for ZnO nanowire LED arrays. In addition, the carrier tunneling process through the MgO layer enables us to investigate carrier transport and light emitting behaviors at low temperature.

In this work, ZnO nanowire LEDs were fabricated and characterized with the presence of an MgO current blocking layer. The EL spectra at various temperatures were analyzed to reveal carrier transport properties in the heterostructure.

The *p*-GaN epilayer was first grown on a *c*-plane sapphire substrate using metal-organic chemical vapor deposition. The effective carrier concentration of the *p*-GaN is approximately 10^{18} cm^{-3}. A 20-nm-thick MgO film was then deposited by rf magnetron sputtering. Next, ZnO nanowire arrays were grown on the MgO film using hydrothermal synthesis in a 100 ml aqueous solution, which contains 10 mM zinc nitrate hexahydrate and 2.5 ml ammonia solution at 95 °C, for 2 h. Figure 1(a) shows the scanning electronic microscopic (SEM) image of the ZnO nanowire arrays. The mesa area of ZnO nanowire arrays is 300×300 μm^2 and was defined using photolithography and diluted HCl etching. The sample was then coated with SiN_x by plasma-enhanced chemical vapor deposition to form an insulating layer and followed by reactive ion etching to remove SiN_x from the nanowire tips. An interesting phenomenon for the SiN_x coated ZnO nanowires is that the upper portion of wires is larger than the bottom part [see Fig. 1(b)]. The unique "inverted trapezoid" profile makes the *n*-type metal connection on top of the nanowires easier to realize. Next, indium–tin–oxide (ITO) layer was then deposited on ZnO nanowire arrays by rf sputtering and was alloyed. Finally, Ni/Au and Ti/Au metal stacks were evaporated on *p*-GaN and ITO, respectively, to complete the device fabrication. The device structure was shown in Fig. 1(c).

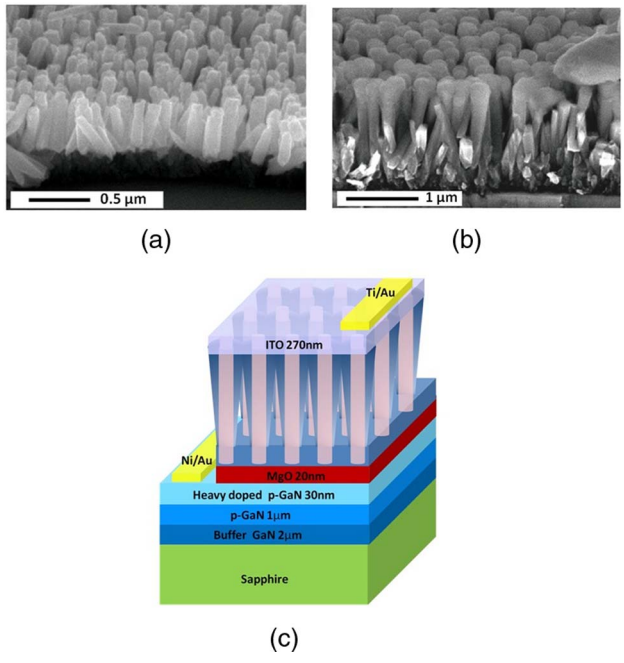

Fig. 1. (Color online) (a) SEM image of the nanowire arrays grown on *p*-GaN/MgO. (b) SEM image of the ZnO nanowire arrays coated with SiN_x. (c) Schematic diagram of ZnO nanowire LED arrays on MgO and *p*-GaN thin films.

We first performed room-temperature photoluminescent (PL) measurement of ZnO nanowire arrays grown directly on a sapphire substrate. The laser excitation wavelength is 266 nm with 5 ps pulse width and 27 kHz repetition rate. The excited spectra were then collected by a fiber and are shown in Fig. 2. The PL spectrum exhibits a sharp near-band-edge emission at 383 nm along with a wide blue-green band emission in the wavelength range around 450 and 550 nm, which has been reported to be associated with oxygen vacancy related defects within the ZnO nanowires as well as in the nanowire surface [11,12].

Next, temperature dependent EL spectra were extracted by placing the sample holder in a vacuum chamber with the ambient temperature controlled by liquid nitrogen flow. The light emission was collected by a fiber. As shown in Fig. 3, at room temperature, the EL spectrum of the device exhibits a dominant sharp emission peak at the wavelength 398 nm, which is mainly attributed to the heterojunction electron-hole recombination and has been discussed previously for planar structure [13]. And the green band light emission is significantly suppressed. As the band diagram sketched in Fig. 4 illustrates, holes and electrons are accumulated in the MgO/*p*-GaN and nanowire ZnO/MgO interfaces, respectively. And radiative recombination occurs as the electrons and holes transport across the MgO barrier through the tunneling process. In particular, owing to the smaller barrier height (1.7 eV) experienced by holes as compared with 3 eV by electrons, holes have more opportunities to tunnel through the MgO barrier and recombine with electrons in the ZnO nanowires.

As we further explore the EL spectra at temperatures from 290 K to 80 K, several interesting phenomena are observed. First, we extract the peak intensity in the UV wavelength range at various temperatures. As demonstrated in Fig. 5(a), the radiation intensity decreases with the temperature until it stabilizes at the temperature below 150–170 K. And, in particular, a sharp decrease is observed at the temperature between 230 K and 200 K. The results can be analyzed by investigating the carrier tunneling process through the MgO barrier layer. First of all, carriers transport across the MgO barrier mainly through the following three processes: Fowler–Nordheim (F-N) tunneling [14], Poole–Frenkel (P-F) tunneling [15], and surface leakage. In the first case, the application of a large electric field results in the tilt of the band structure

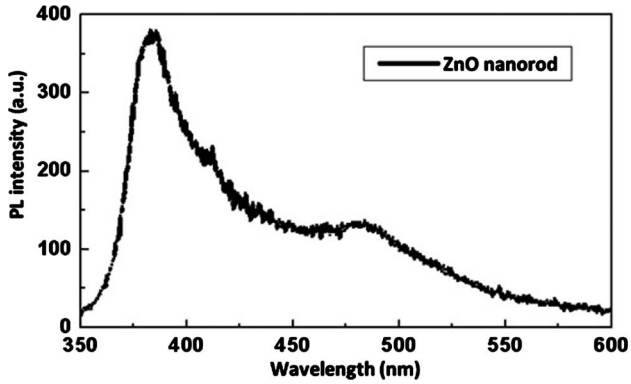

Fig. 2. Room-temperature PL spectrum of ZnO nanowire arrays grown directly on sapphire substrate.

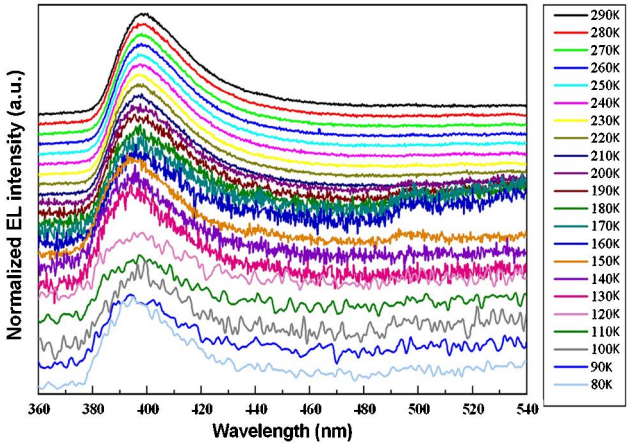

Fig. 3. (Color online) EL spectra of the ZnO nanowire LED arrays at various temperatures.

of MgO toward a triangular profile. The electron-hole transport process can also be accompanied by the P-F tunneling, which is related to the lowering of a Columbic potential barrier when the carriers interact with the traps in the MgO layer. The trapped carriers can therefore hop through the barrier with the help of thermal ionization under the influence of electric field.

At room temperature, carrier transport is dominant by the F-N tunneling with light emission in the near-UV band. Since the F-N tunneling is insensitive to the temperature, at the given constant injection current, the weighting of the P-F effect becomes more significant at low temperature, resulting in the increase of carrier recombination in the MgO defect states. From Fig. 3, the EL intensity in the 480–520 nm wavelength is observed at the temperature between 200 K and 150 K, which is related to the carrier recombination in the MgO defect states. As the temperature is further lower than 160 K, the defect states in the MgO are frozen [16], which implies the mitigation of light emission in

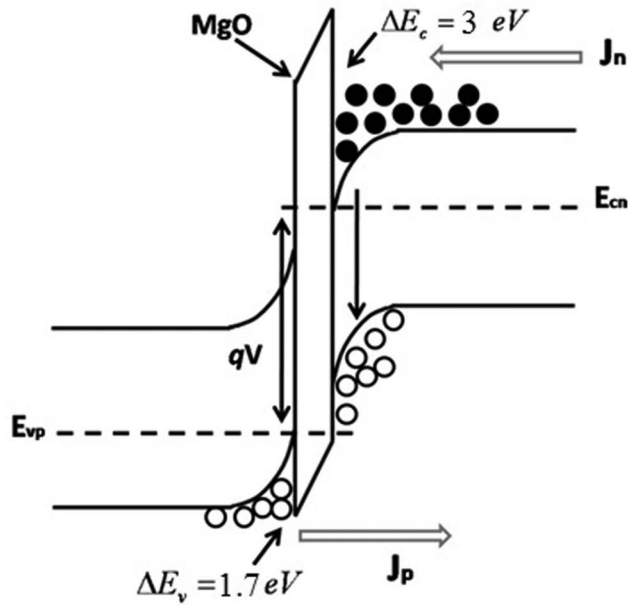

Fig. 4. Band diagram of the ZnO nanowires on MgO and *p*-GaN thin films.

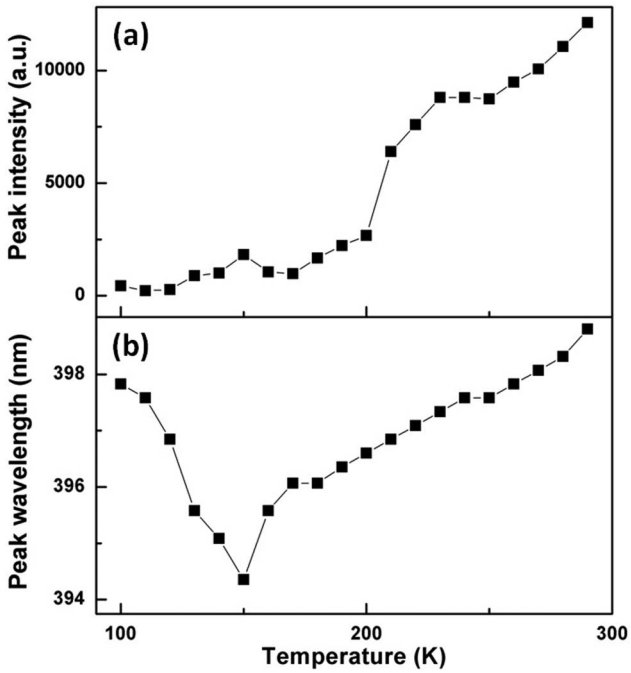

Fig. 5. Temperature dependence of the (a) peak intensity and (b) peak wavelength in the EL spectra.

the 480 nm–520 nm range [17]. And the light output intensity is saturated under 150 K.

Moreover, the peak wavelength at the UV band drifts toward the short wavelength as the temperature is decreased. As illustrated in Fig. 5(b), the peak wavelength reaches its minimum at 150 K and then increases back to 398 nm at 100 K. The effect is associated with the competing factors of the Varshni effect [18] and junction heating [19]. From the Varshni effect, the blueshift of UV emission is related to the temperature-induced bandgap increase. When lowering the temperature from 290 K to 150 K, there will be an increase of 0.06 eV in the bandgap for ZnO nanowires [20] and 0.04 eV for GaN film [21], respectively. Therefore, at 150 K, the bandgaps of ZnO and GaN in the band diagram of Fig. 4 become larger, resulting in the corresponding 0.03 eV blueshift of peak wavelength from 290 K to 150 K. When the temperature drops below 150 K, carrier tunneling becomes difficult as the defect states in MgO and the Mg dopants in the p-GaN are frozen. In such a case, there will be an increase in the device resistivity and the operating voltage. Under a constant current injection, the thermal effect causes band bending and leads to redshift of the peak wavelength.

ZnO nanowire LEDs with the presence of the MgO current blocking layer were characterized. The EL spectra show a significant suppression of defect band light emission, and the high-purity UV light emission at wavelength 398 nm was obtained. As the temperature is decreased, contrary to the typical GaN-based LEDs, our device shows a decrease of optical output intensity. The results are associated with various carrier tunneling processes. While the F-N tunneling is dominant at room temperature, the weighting of P-F tunneling becomes significant at low temperature, leading to MgO defect emission at the wavelength range 480–520 nm. In addition, we observe a blueshift of peak wavelength due to the Varshni effect when the temperature drops from 300 K to 150 K. And the further decrease of temperature results in the redshift due to junction heating.

This work was supported by the National Science Council of Taiwan (NSCT) under the grant NSC97-2221-E-002-054-MY3.

References

1. Y. Leprince-Wang, A. Yacoubi-Ouslim, and G. Wang, Microelectronics J. **36**, 625 (2005).
2. M. Krunks, A. Katerski, T. Dedova, I. Oja Acik, and A. Mere, Solar Energy Mater. Solar Cells **92**, 1016 (2008).
3. C. Lee, T. Lee, S. Lyu, Y. Zhang, H. Ruh, and H. Lee, Appl. Phys. Lett. **81**, 3648 (2002).
4. J. Wang and L. Gao, Solid State Commun. **132**, 269 (2004).
5. Y. Bie, Z. Liao, P. Wang, Y. Zhou, X. Han, Y. Ye, Q. Zhao, X. Wu, L. Dai, and J. Xu, Adv. Mater. **22**, 4284 (2010).
6. O. Lupan, T. Pauporte, and B. Viana, Adv. Mater. **22**, 3298 (2010).
7. O. Lupan, T. Pauporte, B. Viana, I. Tiginyanu, V. Ursaki, and R. Cortes, ACS Appl. Mater. Interfaces **2**, 2083 (2010).
8. W. Weng, S. Chang, C. Hsu, S. Chang, and T. Hsueh, J. Electrochem. Soc. **157**, H866 (2010).
9. J. Sun, Y. Lu, Y. Liu, D. Shen, Z. Zhang, B. Li, J. Zhang, B. Yao, D. Zhao, and X. Fan, J. Phys. D **41**, 155103 (2008).
10. Y. Alivov, J. Van Nostrand, D. Look, M. Chukichev, and B. Ataev, Appl. Phys. Lett. **83**, 2943 (2003).
11. X. Liu, X. Wu, H. Cao, and R. Chang, J. Appl. Phys. **95**, 3141 (2004).
12. W. Park, Y. Jun, S. Jung, and G. Yi, Appl. Phys. Lett. **82**, 964 (2003).
13. C. Chen, M. Ke, C. Liu, Y. Chang, F. Yang, and J. Huang, Appl. Phys. Lett. **91**, 091107 (2007).
14. J. Maserjian and N. Zamani, J. Appl. Phys. **53**, 559 (1982).
15. J. Yeargan and H. Taylor, J. Appl. Phys. **39**, 5600 (1968).
16. X. Cao, S. LeBoeuf, L. Rowland, C. Yan, and H. Liu, Appl. Phys. Lett. **82**, 3614 (2003).
17. J. Zhang and L. Zhang, Chem. Phys. Lett. **363**, 293 (2002).
18. Y. Varshni, Physica **34**, 149 (1967).
19. Y. Li, W. Fang, W. Liu, H. Liu, C. Mo, L. Wang, and F. Jiang, J. Lumin. **122**, 567 (2007).
20. X. Zhang, S. Chua, A. Yong, H. Yang, S. Lau, S. Yu, X. Sun, L. Miao, M. Tanemura, and S. Tanemura, Appl. Phys. Lett. **90**, 013107 (2007).
21. Y. Li, Y. Lu, H. Shen, M. Wraback, M. Brown, M. Schurman, L. Koszi, and R. Stall, Appl. Phys. Lett. **70**, 2458 (1997).